LOSSLESS COMPRESSION OF CFA SAMPLED IMAGE USING DECORRELATED MALLAT WAVELET PACKET DECOMPOSITION

Yeejin Lee[⋆]*, Keigo Hirakawa*[†]*, and Truong Q. Nguyen*[⋆]

[⋆] ECE Dept., University of California San Diego, La Jolla, CA 92093
[†] ECE Dept., University of Dayton, Dayton, OH 45469

ABSTRACT

This paper presents a rigorous analysis of wavelet transform on color filter array (CFA) sampled images. The presented analysis suggests that the wavelet coefficients of *HL* and *LH* subbands are highly correlated. Hence, we propose a novel lossless compression scheme for CFA sampled images using the decorrelated Mallat wavelet packet decomposition. We validated our theoretical analysis and the performance of the proposed compression scheme using images of natural scenes captured in a raw format. The experimental results verify that our proposed method improves coding efficiency relative to the standard and the state-of-the-art lossless compression schemes CFA sampled images.

Index Terms— Color filter array, image compression, lossless coding, camera processing pipeline, wavelet transform, JPEG

1. INTRODUCTION

Color filter array refers to a spatial multiplexing of red, green, and blue filters over the image sensor surface. The raw sensor data captured by this configuration is therefore a subsampled version of a full color image, where each pixel measures the intensity of only a red, green, or blue value. Demosaicking process interpolates the raw image and recovers the full color image representation. Besides demosaicking, the captured data undergo defective sensor pixel removal, color correction, gamma correction, noise suppression, etc. Once the camera processing pipeline renders the color image, an image compression algorithm transforms the processed image to a storage format that requires fewer pixels. In most cases, the compression is lossy.

Professional photographers and photo enthusiasts however prefer to work directly with the raw sensor data to gain maximum control over the postprocessing. In such applications, it is desirable to leave raw sensor data uncompressed to ensure maximum image quality. However, the storage requirement is large, and lossless compression is highly desirable. At the same time, compressing the raw sensor data directly has the potential to improve compression performance relative to working with a full color image. Despite the fact that the color images requires more bits to encode all color components, compression of CFA sampled images has received very limited attention in the literature [1–8].

To this end, we propose a novel lossless compression scheme for raw sensor data. Our work is inspired by the CFA compression method of [1], the wavelet sampling theory of [9], and the demosaicking work of [10]. Specifically, the lossless CFA sampled image compression scheme in [1] leveraged a heuristic observation made on the Mallat wavelet packet transform coefficients of the sampled image. A more rigorous analysis of wavelet sampling in [9] reveals that Mallat wavelet coefficients are highly redundant. We previously used this fact to develop demosaicking [10–12] and denoising [11]. In this paper, we use it to further decorrelate the Mallat coefficients in order to improve the lossless compression of CFA sampled images.

The remainder of the paper is organized as follows. In Section 2, we provide a wavelet analysis of CFA sampled images. The proposed compression method is developed in Section 3. Experimental results are shown in Section 4 before making concluding remark in Section 5.

2. BACKGROUND AND REVIEW

In [1], it was empirically observed that the one-level wavelet transform of a CFA sampled image was predominantly lowpassed. Indeed, there is a profound difference between the LeGall 5/3 wavelet transform of a CFA sampled image shown in Fig. 1(c) and the wavelet transform of a luminance image in Fig. 1(b). Specifically, the wavelet subbands (i.e. *LH*, *HL*, and *HH*) in Fig. 1(c) are not sparse, unlike the highly compressible highpass components in Fig. 1(b). The work in [1] therefore proposed a Mallat wavelet packet decomposition to sparsify the wavelet coefficients with additional multiresolution analysis.

The work in [9, 10] provided a rigorous analysis of Fig. 1(c), which we review here. Let $\boldsymbol{x}(\boldsymbol{n}) = [r(\boldsymbol{n})\ \ g(\boldsymbol{n})\ \ b(\boldsymbol{n})]^T$ be a color image where $r(\boldsymbol{n})$, $g(\boldsymbol{n})$, and $b(\boldsymbol{n})$ represent the red, green, and blue color components, respectively. Then the CFA sampled data $y(\boldsymbol{n})$ at pixel location $\boldsymbol{n} = [n_0\ \ n_1]^T$ is [12]

$$\begin{aligned} \boldsymbol{y}(\boldsymbol{n}) &= \boldsymbol{c}(\boldsymbol{n})^T \boldsymbol{x}(\boldsymbol{n}) \\ &= g(\boldsymbol{n}) + c_r(\boldsymbol{n})\alpha(\boldsymbol{n}) + c_b(\boldsymbol{n})\beta(\boldsymbol{n}), \end{aligned} \tag{1}$$

where α and β defined as $\alpha(\boldsymbol{n}) = r(\boldsymbol{n}) - g(\boldsymbol{n})$ and $\beta(\boldsymbol{n}) = b(\boldsymbol{n}) - g(\boldsymbol{n})$ are taken to be proxies for chrominance images; and the vector $\boldsymbol{c}(\boldsymbol{n}) = [c_r(\boldsymbol{n})\, c_g(\boldsymbol{n})\, c_b(\boldsymbol{n})]^T \in \{0,1\}^3$ is a sampling lattice (e.g. $\boldsymbol{c}(\boldsymbol{n}) = [1\ \ 0\ \ 0]$ denotes a red pixel at pixel location $\boldsymbol{n}$). The CFA sampled image of (1) is composed of luminance component (fully observed green pixels) and chrominance components (sparsely sampled color differences). The advantage to such decomposition is that α and β are lowpass signals [13].

The first level wavelet transform of $y(\boldsymbol{n})$ is [9, 14]:

$$w^y_{i,j}(\boldsymbol{n}) = w^g_{i,j}(\boldsymbol{n}) + w^{c_r\cdot\alpha}_{i,j}(\boldsymbol{n}) + w^{c_b\cdot\beta}_{i,j}(\boldsymbol{n}), \tag{2}$$

where w^c denotes the wavelet coefficient for components c (e.g. $c = g$), and the subband index $(i,j) \in \{L,H\}^2$ denotes lowpass (L) and highpass (H) in the vertical and horizontal directions.

Let L^* and H^* denote subbands of conjugate wavelet transform coefficients computed using conjugated wavelet filters, as described in [9]. Approximating the detail coefficients of chrominance by

(a) (b) Ordinary wavelet (c) CFA wavelet (d) (e) Decorrelated CFA wavelet

Fig. 1. Comparison of the one-level LeGall 5/3 wavelet transforms. (b) Wavelet coefficients of a luminance image. (c) Wavelet coefficients of a CFA sampled image. (e) Wavelet coefficients of a CFA sampled image with decorrrelation. The subbands layout for (b) and (c) is shown in (a); the layout for (e) is shown in (d). Note that the coefficient magnitudes are scaled for display.

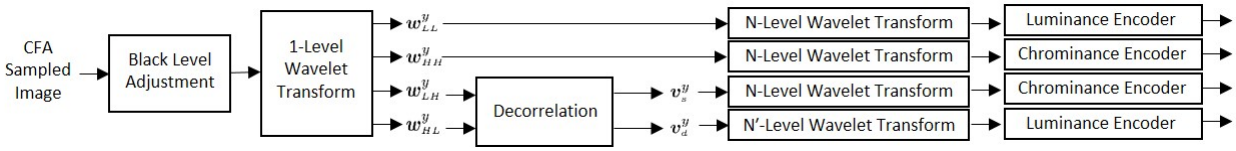

Fig. 2. Description of the proposed decorrelated Mallat wavelet packet decomposition.

zero (i.e. $w^{\alpha}_{i,j}(\boldsymbol{n}) = w^{\beta}_{i,j}(\boldsymbol{n}) = 0$ for $(i,j) \neq \{L, L\}$), the wavelet transform in (2) can be rewritten as [10, 11]

$$\begin{aligned} w^y_{LL}(\boldsymbol{n}) &= w^g_{LL}(\boldsymbol{n}) + {}^1\!/_4 w^{\alpha}_{LL}(\boldsymbol{n}) + {}^1\!/_4 w^{\beta}_{LL}(\boldsymbol{n}) \\ w^y_{LH}(\boldsymbol{n}) &= w^g_{LH}(\boldsymbol{n}) + {}^1\!/_4 w^{\alpha}_{LL^*}(\boldsymbol{n}) - {}^1\!/_4 w^{\beta}_{LL^*}(\boldsymbol{n}) \\ w^y_{HL}(\boldsymbol{n}) &= w^g_{HL}(\boldsymbol{n}) + {}^1\!/_4 w^{\alpha}_{L^*L}(\boldsymbol{n}) - {}^1\!/_4 w^{\beta}_{L^*L}(\boldsymbol{n}) \\ w^y_{HH}(\boldsymbol{n}) &= w^g_{HH}(\boldsymbol{n}) + {}^1\!/_4 w^{\alpha}_{L^*L^*}(\boldsymbol{n}) + {}^1\!/_4 w^{\beta}_{L^*L^*}(\boldsymbol{n}). \end{aligned} \tag{3}$$

Hence, the wavelet coefficients of the CFA sampled image are interpreted as a linear combination of the coefficients of luminance and the lowpass coefficients of chrominance. This fact can be confirmed by Fig. 1(c) where *LH*, *HL*, and *HH* subbands are dominanted by lowpass components α and β (rather than the highpass components, as in the case of Fig. 1(b)).

3. PROPOSED LOSSLESS COMPRESSION OF CFA SAMPLED IMAGE

The schematic representation of the proposed compression method is shown in Fig. 2. The analysis in Section 2 demonstrates that each one-level wavelet subband of the CFA sampled image combines low frequency of chrominance and high frequency of luminance components. Lowpass components yield poor compression efficiency because their coefficients are not sparse. Even if decomposed further by subsequent wavelet transforms [1], the coefficients $w^{\alpha}_{LL^*}$, $w^{\alpha}_{L^*L}$, $w^{\beta}_{LL^*}$, and $w^{\beta}_{L^*L}$ would never achieve the compression rate of w^g_{HL} and w^g_{LH} because the latter are of a finer scale wavelet transform.

We propose to decorrelate the w^g_{HL} and w^g_{LH} by orthogonal transformation using the bases $[1 \;\; 1]^T$ and $[-1 \;\; 1]^T$. Examining (3) further, $w^{\alpha}_{LL^*}$ in w^y_{LH} and $w^{\alpha}_{L^*L}$ in w^y_{HL} are the transforms of the same chrominance image α using two different wavelet types. As such, they are highly correlated, as evidenced by $w^{\alpha}_{LL^*}$ plotted against $w^{\alpha}_{L^*L}$ in Fig. 3(a). The strength of correlation as indicated by the Pearson moment correlation coefficient is 0.9989. The same relation holds for $w^{\beta}_{LL^*}$ and $w^{\beta}_{L^*L}$. In the proposed method, we

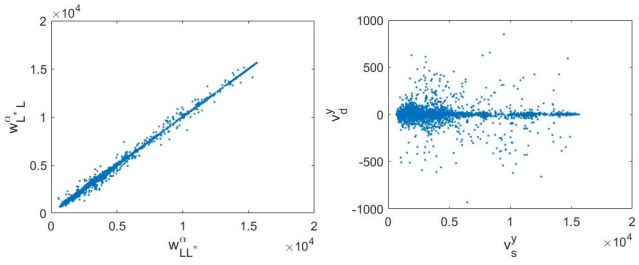

(a) (b)

Fig. 3. Illustration of high redundancy in Mallat wavelet decomposition. (a) Plot of $w^{\alpha}_{LL^*}$ against $w^{\alpha}_{L^*L}$. (b) Plot of v^y_s against v^y_d.

replace w^y_{HL} and w^y_{LH} by the decorrelated coefficients of the form:

$$\begin{aligned} v^y_d(\boldsymbol{n}) &= w^y_{LH}(\boldsymbol{n}) - w^y_{HL}(\boldsymbol{n}) = w^g_{LH}(\boldsymbol{n}) - w^g_{HL}(\boldsymbol{n}) \\ &\quad + {}^1\!/_4 \Big(w^{\alpha}_{LL^*}(\boldsymbol{n}) - w^{\alpha}_{L^*L}(\boldsymbol{n}) \Big) - {}^1\!/_4 \Big(w^{\beta}_{LL^*}(\boldsymbol{n}) - w^{\beta}_{L^*L}(\boldsymbol{n}) \Big), \\ v^y_s(\boldsymbol{n}) &= \Big\lfloor \tfrac{1}{2} \left(w^y_{LH}(\boldsymbol{n}) + w^y_{HL}(\boldsymbol{n}) \right) \Big\rfloor \\ &= \Big\lfloor \tfrac{1}{2} \Big\{ w^g_{LH}(\boldsymbol{n}) + w^g_{HL}(\boldsymbol{n}) + {}^1\!/_4 \Big(w^{\alpha}_{LL^*}(\boldsymbol{n}) + w^{\alpha}_{L^*L}(\boldsymbol{n}) \Big) \\ &\quad - {}^1\!/_4 \Big(w^{\beta}_{LL^*}(\boldsymbol{n}) + w^{\beta}_{L^*L}(\boldsymbol{n}) \Big) \Big\} \Big\rfloor, \end{aligned}$$

where $\lfloor \cdot \rfloor$ denotes a *floor* operation. The coefficients $w^y_{LH}(\boldsymbol{n})$ and $w^y_{HL}(\boldsymbol{n})$ are perfectly reconstructable from v^y_d and v^y_s by the relation:

$$\begin{aligned} w^y_{HL}(\boldsymbol{n}) &= v^y_s(\boldsymbol{n}) - \Big\lfloor \tfrac{v^y_d(\boldsymbol{n})}{2} \Big\rfloor, \\ w^y_{LH}(\boldsymbol{n}) &= v^y_d(\boldsymbol{n}) + w^y_{HL}(\boldsymbol{n}). \end{aligned} \tag{4}$$

The difference subband v^y_d is designed to decorrelate $w^{\alpha}_{LL^*}$ and $w^{\alpha}_{L^*L}$ ($w^{\beta}_{LL^*}$ and $w^{\beta}_{L^*L}$, also). This fact is confirmed by Fig. 3(b)

(a) Test images of Nikon D810

(b) Test images of Sony Alpha a7R II

Fig. 4. Raw sensor images used in our experiments. Source is `www.imaging-resource.com`, reproduced with a written permission.

and by the fact that correlation coefficient reduces to -0.0378. In fact, one can show that the difference $w^{\alpha}_{LL^*} - w^{\alpha}_{L^*L}$ represents a bandpass transform of the lowpass signal α (and similarly with β) by a filter $LL^* - L^*L$, which is very small. We conclude that the decorrelated coefficient v^y_d is comprised of bandpass components $w^{\alpha}_{LL^*} - w^{\alpha}_{L^*L}$ and $w^{\beta}_{LL^*} - w^{\beta}_{L^*L}$; and a highpass component $w^g_{LH} - w^g_{HL}$. Hence, it requires only minimal additional levels (N' in Fig. 2) of wavelet transforms (LeGall 5/3 in our implementation) to sparsify v^y_d. We subsequently encode the transformed v^y_d by the luminance highpass encoding scheme (since v^y_d dominated by w^g_{HL} and w^g_{LH}), and we expect a coding efficiency comparable to the fine level wavelet transform coefficients w^g_{HL} to be w^g_{LH}.

On the other hand, the sum subband v^y_s represents a combination of lowpass components of α and β by a filter $LL^* + L^*L$, which is also lowpass component. Hence, the wavelet coefficient v^y_s is dominated by the chrominance w^{α}_{LL} and w^{β}_{LL} and thus should be treated like a chrominance image. In a manner similar to the Mallat wavelet packet analysis of [1], we proposed to apply additional LeGall 5/3 wavelet transform to decompose this further. The N-level wavelet transform of v^y_s is encoded (where $N \gg N'$) by the lossless encoding scheme for the chrominance component.

Finally, w^y_{LL} and w^y_{HH} in (3) play the roles of lowpass luminance and chrominance, respectively. Hence, additional wavelet decompostions, similar to the approach of [1], are applied. An N-level Mallat wavelet packet transforms of w^y_{LL} and w^y_{HH} are encoded by luminance and chrominance encoders, respectively.

In wavelet-based compression schemes such as JPEG2000, the coding efficiency increases as more coefficients are concentrated near zero. In order to distribute coefficients around zero, each color component of the CFA sampled image is shifted by adjusting its offset before taking wavelet transform, as follows:

$$\boldsymbol{y}'(\boldsymbol{n}) = \boldsymbol{y}(\boldsymbol{n}) - \boldsymbol{k} \tag{5}$$

where $\boldsymbol{k} = [k_r\ k_g\ k_b]^T$ is the integer offset values of color components. The shift $\boldsymbol{k}$ must be stored as a sideband information in order to uncompress the image later. In the experiment, the values are chosen by black offset, which was computed from a calibration experiment using X-Rite ColorChecker[1].

4. EXPERIMENTAL RESULTS

We verified our proposed method using 30 raw sensor images of Nikon D810 and Sony Alpha a7R II as shown in Fig. 4. Those cameras are especially challenging to work with because they lack the optical lowpass filters. (We did not consider the low-resolution Kodak and IMAX images typically used in demosaicking and compression studies, as the resolution of typical modern digital cameras far exceeds them.) In the proposed method, the transformed images were coded using the standard JPEG2000 codec, *openJPEG*[2]. The level of wavelet transformation was set to 5 (i.e. $N = 4$ and $N' = 1$ in Fig. 2), which is the default setting of *openJPEG*. The size of a code block was set to 64×64 as a default value. The raw sensor data was cropped to the size 4436×6642 (Nikon) and 4788×7200 (Sony) because of the size limitation of the openJPEG engine.

For comparison, we decomposed the color images and the raw images using LeGall 5/3 wavelet transform for lossless coding of JPEG2000 in different configurations. They are: the wavelet transform on the color images reconstructed in a typical image processing pipeline (denoted as *RGB* in Table 1), the wavelet transform on the CFA sampled images treated as gray images (*CFA*), the wavelet transform on the demultiplexed color images at low resolution (*Demux*), the macropixel spectral-spatial transformation (*MSST*) on the CFA sampled images [3], and the Mallat wavelet packets transformation on the CFA sampled images (*Mallat*) [1].

The compression results are tabulated in Table 1 in terms of bits per pixel (bpp). It is important to note that all of the experiments are conducted using a standard JPEG2000 codec, and so the only difference among the methods compared in Table 1 is the wavelet decomposition schemes applied. The relative compression gain of the proposed method is also presented in the table. Our proposed method improves coding efficiency by about 3% (Nikon) and 14% (Sony) relative to the standard JPEG2000 coding. Since the total number of pixel components being coded is three times than that of a CFA sampled image in the standard JPEG2000 coding, the RGB encoding is obviously the least efficient. The large coding gain of Sony camera stems from the fact that the dynamic range of raw data was close to 2^{13} while the processed color image exceeded 2^{13} requiring an extra bit of representation. Typically, the dynamic range of the color images are increased through the camera processing pipeline if raw data are dark, and so this is not entirely unexpected. Relative to directly applying JPEG2000 lossless compression to CFA sampled images, we gained 5.19% (Nikon) and 6.03% (Sony). This can be explained by Fig. 1(b), which shows that the *HL*, *LH*, and *HH* subbands are dominated by non-sparse chrominance components. Relative to the demultiplexing method, the MSST and the Mallat wavelet transform compression scheme improved by about 1% (Nikon) and 0.5% (Sony). The proposed scheme improved fur-

[1] `www.xritephoto.com`

[2] `www.openjpeg.org`

Table 1. The comparison of bits per pixel (bpp) for different decomposition methods. The bit depth of the raw sensor readout for both cameras is 14 bits. The coding gain of the proposed method with respect to the other methods is computed as *(bpp of other methods - bpp of our method)/bpp of other methods* in percentage.

Images	Nikon D810						Sony Alpha a7R II					
	RGB	*CFA*	*Demux*	*MSST*	*Mallat*	*Ours*	*RGB*	*CFA*	*Demux*	*MSST*	*Mallat*	*Ours*
1	7.183	6.809	6.540	6.454	6.433	**6.410**	7.437	6.801	**6.292**	6.328	6.318	6.305
2	7.685	7.888	7.665	7.601	7.575	**7.535**	7.130	6.434	6.032	5.981	5.979	**5.964**
3	7.920	7.324	7.097	**7.096**	7.124	7.124	7.112	6.554	6.202	6.135	6.109	**6.083**
4	7.657	8.033	7.802	7.733	7.705	**7.654**	7.719	7.140	6.923	6.889	6.856	**6.798**
5	8.218	8.832	8.442	8.404	8.402	**8.387**	6.827	6.056	5.688	5.636	5.648	**5.621**
6	7.691	8.348	8.121	8.011	7.977	**7.947**	7.096	6.660	6.298	6.226	6.220	**6.199**
7	7.475	7.430	6.943	6.924	6.930	**6.922**	7.196	6.230	**5.731**	5.789	5.845	5.807
8	8.276	8.083	7.913	7.856	7.819	**7.800**	7.145	6.077	5.670	**5.619**	5.661	5.622
9	9.543	8.838	8.989	8.795	8.692	**8.624**	7.397	6.817	6.547	6.461	6.466	**6.423**
10	6.789	7.987	7.341	7.366	7.344	**7.338**	8.928	7.967	**7.766**	7.789	7.814	7.800
11	7.591	8.964	8.542	8.545	8.501	**8.468**	6.580	6.175	**5.546**	5.559	5.573	5.562
12	7.803	8.099	7.690	7.671	7.655	**7.643**	7.428	8.169	7.820	7.814	7.799	**7.794**
13	7.195	7.022	6.820	6.783	6.778	**6.311**	9.415	7.477	7.479	7.351	7.272	**7.207**
14	8.579	8.505	8.217	8.203	8.188	**8.173**	7.201	7.883	7.338	7.317	7.267	**7.249**
15	7.197	7.371	7.224	7.077	7.030	**6.989**	8.513	7.344	**7.077**	7.082	7.100	7.088
Average	7.787	7.969	7.690	7.635	7.610	**7.555**	7.541	6.919	6.561	6.532	6.529	**6.502**
Our Gain	2.98%	5.19%	1.75%	1.05%	0.72%	–	13.79%	6.03%	0.90%	0.46%	0.41%	–

ther by 1.05% (Nikon) and 0.46% (Sony) relative to the MSST; and 0.72% (Nikon) and 0.41% (Sony) relative to the Mallat wavelet scheme. The bpps in Table 1 validate our theoretical analysis in Section 3 that the decorrelated Mallat wavelet packet transform on CFA sampled images reduces bit requirement.

The total processing time is dominated by the wavelet transformation and the variable length coding. We only require wavelet transform of a CFA sampled image at the first level, which is one-third the complexity of the JPEG2000 for color images. The decorrelation requires only an addition and a subtraction, which is a negligible overhead. The subsequent N-dimensional wavelet transform is applied three times, comparable to JPEG2000 for color images (after the first level wavelet decomposition); and requires $3/4$ complexity relative to [1]. The number of wavelet coefficients that are encoded by the variable length encoder is a third of the JPEG2000. Hence, we conclude that the proposed method is substantially less complex than the conventional JPEG2000 and slightly less than [1].

Finally, a Golomb-Rice coding scheme (the code not publicably available) was used in [1] instead of the JPEG2000 lossless encoder. While this provided additional bit rate improvement, we expect similar benefits to the proposed scheme as well if such coding scheme was used on v_d^y and v_s^y. See [2, 5] for studies along this line.

5. CONCLUSION

This paper introduced a lossless compression scheme for raw sensor data, leveraging the decorrelated Mallat wavelet transform to generate sparse wavelet coefficients. In addition to proposing a new scheme for compressing raw sensor data, the analysis on the wavelet transform of CFA sampled image was presented. The experimental results verified that the proposed method improves coding efficiency compared to the standard and the state-of-the-art lossless CFA sampled image compression schemes.

6. ACKNOWLEDGMENT

We thank the staff at Image Resource for giving us the permission to reproduce the raw sensor images used in this study. We also thank openJPEG for the encoding scheme we used to produce Table 1.

7. REFERENCES

[1] N. Zhang and X. Wu, "Lossless compression of color mosaic images," *IEEE Trans. Image Process.*, vol. 15, pp. 1379–1388, May 2006.

[2] K.-H. Chung and Y.-H. Chan, "A lossless compression scheme for bayer color filter array images," *IEEE Trans. Image Process.*, vol. 17, pp. 134–144, January 2008.

[3] H. S. Malvar and G. J. Sullivan, "Progressive-to-lossless compression of color-filter-array images using macropixel spectral-spatial transformation," in *Data Compress. Conf. (DCC)*. IEEE, 2012, vol. 1, pp. 3–12.

[4] D. Lee and K. N. Plataniotis, "A novel high dynamic range image compression scheme of color filter array data for the digital camera pipeline," in *Int. Conf. Image Process. (ICIP)*. IEEE, 2012, vol. 1, pp. 325–328.

[5] S. Kim and N. Cho, "Lossless compression of color filter array images by hierarchical prediction and context modeling," *IEEE Trans. Circuits Syst. Video Technol.*, vol. 24, pp. 1040–1046, January 2014.

[6] C.-H. Lin, K.-L. Chung, and C.-W. Yu, "Novel chroma subsampling strategy based on mathematical optimization for compressing mosaic videos with arbitrary rgb color filter arrays in H.264/AVC and HEVC," *IEEE Trans. Circuits Syst. Video Technol.*, vol. 26, no. 9, pp. 1722–1733, Sept. 2016.

[7] M. Lakshmia, J. Senthilkumarb, and Y. Sureshb, "Visually lossless compression for bayer color filter array using optimized vector quantization," *Applied Soft Comput.*, vol. 46, pp. 1030–1042, Sept. 2016.

[8] A. Trifan and A. J. R. Neves, "A survey on lossless compression of bayer color filter array images," *Int. J. of Computer, Electrical, Autom., Control and Informat. Eng.*, vol. 10, no. 4, pp. 729–734, Nov. 2016.

[9] K. Hirakawa and P. J. Wolfe, "Rewiring filterbanks for local fourier analysis: Theory and practice," *IEEE Trans. Inf. Theory*, vol. 57, pp. 5360 – 5374, July 2011.

[10] J. T. Korneliussen and K. Hirakawa, "Camera processing with chromatic aberration," *IEEE Trans. Image Process.*, vol. 23, pp. 4539–4552, August 2014.

[11] K. Hirakawa, X.-L Meng, and P. J. Wolfe, "A framework for wavelet-based analysis and processing of color filter array images with applications to denoising and demosaicing," in *Int. Conf. Acoust., Speech, Signal Process. (ICASSP)*. IEEE, 2007, vol. 1, pp. 597–600.

[12] D. Alleysson, S. Susstrunk, and J. Herault, "Linear demosaicing inspired by the human visual system," *IEEE Trans. Image Process.*, vol. 14, pp. 439–449, March 2005.

[13] B. K. Gunturk, J. Glotzbach, Y. Altunbasak, R. W. Schafer, and R. M. Mersereau, "Demosaicking: color filter array interpolation," *IEEE Signal Process. Mag.*, vol. 22, pp. 44–54, March 2005.

[14] J. Gu, P. J. Wolfe, and K. Hirakawa, "Filterbank-based universal demosaicking," in *Int. Conf. Image Process. (ICIP)*. IEEE, 2010, vol. 1, pp. 1981–1984.